Catalysis Today 146 (2009) 96–102

Contents lists available at ScienceDirect

Catalysis Today

journal homepage: www.elsevier.com/locate/cattod

# Disk-type porous Ni–Cr bulk catalyst for hydrogen production by autothermal reforming of methane

Sung Ho Kim [a], Ji Hye Chung [a], Yun Tae Kim [a], Jonghee Han [b], Sung Pil Yoon [b], Suk-Woo Nam [b], Tae-Hoon Lim [b], Ho-In Lee [a,*]

[a] School of Chemical and Biological Engineering & Research Center for Energy Conversion and Storage, Seoul National University, 599 Gwanangno, Gwanak-gu, Seoul 151-744, Republic of Korea
[b] Center for Fuel Cell Research, Korea Institute of Science and Technology, 39-1 Hawolgok-dong, Sungbuk-gu, Seoul 136-791, Republic of Korea

ARTICLE INFO

*Article history:*
Available online 23 February 2009

*Keywords:*
Disk-type catalyst
Ni bulk catalyst
ATR
Methane reforming
On–Off test

ABSTRACT

Autothermal reforming of methane, which is combined of steam reforming and partial oxidation, was carried out with a disk-type porous Ni–Cr bulk catalyst in various reaction conditions. Although high methane conversion could be obtained by controlling reaction conditions such as reaction temperature, $O_2$/C ratio, and S/C ratio, the optimal condition for maximal $H_2$ and CO generation was shown at a different reaction condition, because $H_2$ and CO were products of partially oxidized methane. The activity of porous Ni–Cr bulk catalyst was well maintained for On–Off test and 260 h operation of ATR. The deactivation of a reforming catalyst has generally been caused by the carbon deposition on the active site of Ni. In the case of bulk Ni, however, the oxidation of Ni was an inevitable and severe problem in the autothermal reforming of methane. An interesting fact was observed during On–Off test, which was named a bounce phenomenon in this work. It was caused by oxidation of Ni for On–Off process and the transient reduction of the oxidized Ni catalyst in ATR reaction.

## 1. Introduction

Efficient syngas generation technology was a necessity for commercial Fischer–Tropsch (FT) synthesis [1,2]. In recent years, however, there has been much interested in the production of hydrogen for high efficient electricity generation by fuel cells. Fuel cell is an energy-conversion device that produces electricity directly by electrochemical combination of hydrogen and oxygen [3]. Compared to an internal combustion, the fuel cell system works more efficiently and produces less emission [4].

### 1.1. Autothermal reforming of methane

The lack of infrastructure for hydrogen production and the unsolved hydrogen storage problem are accelerating the development of compact fuel reformers that are able to produce a hydrogen-rich syngas from hydrocarbons. Methane (the main constituent of natural gas), due to its large abundance and high H:C ratio, has been recognized as an ideal fuel source for hydrogen production. Methane can also be obtained from biomass, which the amount is similar with the output of yearly oil production in the world [5,6]. Biomass may be converted to various energy forms such as heat, steam, hydrogen, methanol, and methane. Under most circumstances, methane is an ideal product because infrastructure of pipe line and hardware is well-equipped.

To produce hydrogen by reforming methane, it should be processed under very severe conditions because it is very stable molecule. Although its conversion to syngas can be conducted at reaction temperatures even below 700 K, higher temperature is substantially needed to obtain high hydrogen yield, typically 1100 K. There are two main reactions for methane reforming processes: (1) steam reforming (SR) [7–9] and (2) partial oxidation (POX) [7,8]. SR (1) is a highly endothermic reaction of methane and steam, whereas POX (2) is slightly exothermic:

$$\text{SR}:\ CH_4 + H_2O \rightarrow CO + 3H_2 \quad (\Delta H^\circ = 206\,\text{kJ/mol}) \tag{1}$$

$$\text{POX}:\ CH_4 + 0.5O_2 \rightarrow CO + 2H_2 \quad (\Delta H^\circ = -36\,\text{kJ/mol}) \tag{2}$$

Autothermal reforming (ATR) (3) [10–12], which is a combination of (1) and (2), is an alternative approach to product syngas:

$$\text{ATR}:\ CH_4 + aH_2O + bO_2 \rightarrow xCO + yH_2 + zCO_2 \quad (\Delta H^\circ = 0\,\text{kJ/mol}) \tag{3}$$

Reaction (3) is considered as thermally self-sustaining reaction [13,14]. Therefore, we can reduce external energy supplying into a reforming reaction.

---

* Corresponding author. Tel.: +82 2 880 7072; fax: +82 2 888 1604.
*E-mail address:* hilee@snu.ac.kr (H.-I. Lee).

0920-5861/$ – see front matter © 2009 Elsevier B.V. All rights reserved.
doi:10.1016/j.cattod.2009.01.042

### 1.2. Disk-type porous Ni–Cr bulk catalyst

Catalytic ATR of methane over supported metal catalysts have been investigated in the present study [15]. The sequence of an activity of catalyst has been reported as Rh > Pd > Ni > Pt > Co for ATR reaction [14]. This activity sequence is widely agreed with the reported activities for steam reforming. Rh catalyst attains the highest activity, but Ni is much cheaper catalyst than noble one. Ni has been more used in real process than noble catalysts. However, it has many shortcomings such as easy sintering problem at high temperature and inevitable deactivation by coke formation [16–18]. Moreover, the reactor manufactured with supported Ni has a large reactor volume by catalyst volume. It is unreasonable to manufacture small scale reformer for applying on-board fuel cell system.

For that reason, porous Ni bulk catalyst was prepared to reduce the reactor volume, but the catalyst prepared as reforming catalyst was physically unstable. When porous Ni bulk catalyst was prepared by only Ni metal powder, its activity decreased rapidly due to physical instability. So, porous Ni bulk catalyst is not effective in reforming. To improve the catalyst stability, Cr was added to Ni bulk metal, and the catalyst showed thermal and structural stability in reforming condition. In the present work, disk-type porous Ni–Cr bulk catalyst is suggested as an effective and optimal catalyst for ATR reaction.

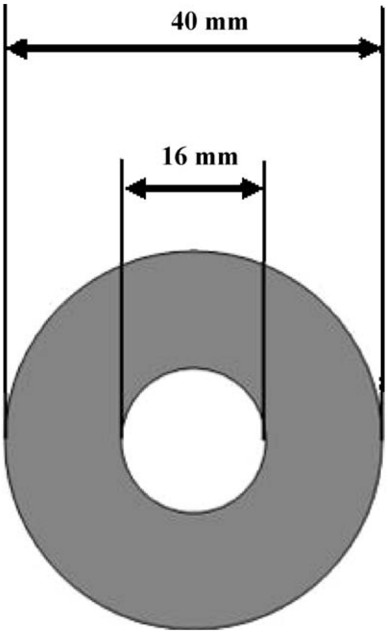

**Fig. 1.** A shape of disk-type porous Ni–Cr bulk catalyst.

## 2. Experimental

### 2.1. Preparation of disk-type porous Ni–10 wt% Cr bulk catalyst

The slurry, a mixture of solvent (water), binder (Methyl Cellulose #1,500, Junsei Chemical Co., Japan), plasticizer (Glycerol, Junsei Chemical Co., Japan), defoamer (SN-154, San Nopco Korea), deflocculant (Cerasperse-5468, San Nopco Korea), dispersant (polyacrylic acid) Ni metal powder (INCO. #255, INCO) and Cr metal powder (CR-102, ATLANTIC EQUIPMENT ENGINEERS) [19] is ball milled for a period of 15 h, first. The second ball milling for 6 h was carried out after addition of polyethylene oxide to the first ball milling slurry. And then, a very small amount of methyl cellulose, sodium carboxyl methyl cellulose as binder, and isopropyl alcohol as deairing agents were added to the second ball milled slurry and the third ball milling was conducted for 1 h. In order to eliminate the air from this third ball milled slurry, a vacuum pump and stirring equipment were used. Green sheet is made by use of a doctor blade in which tapecasting was done with deairing slurry and drying sufficiently at ambient temperature. Ni–Cr green sheet was sintered at 1000 °C with $H_2$/Ar atmosphere. And then, sintered Ni–Cr bulk catalyst was cut out with disk type of 16 mm inner diameter and 40 mm outer diameter by laser. The thickness of Ni–Cr disk was ca. 0.75 mm, porosity measured by mercury porosimeter was ca. 50%. Fig. 1 shows the shape of disk-type Ni–Cr catalyst.

### 2.2. Reactor and reaction system

The reactor for autothermal reforming was made of stainless steel to sustain high temperature. Mixed gas of methane, air, and steam entered vertically inside the disk-type catalyst, and flowed in parallel over the surface of the disk-type catalyst for reaction test as shown in Fig. 2, which shows the inside of reactor and the schematic diagram for the flow direction of the mixed gas. Inconel sheets above and below the disk-type catalyst were equipped for a role of flow path. That is, the catalyst was placed between the Inconel sheets. And also, the catalyst layer containing the disk-type catalyst and Inconel sheets was fixated by stainless steel plate. An electric furnace for performance test was used and a thermocouple (K-type) was put inside the disk-type catalyst to measure the reaction temperature.

The flow rate of methane and air was controlled by mass flow controller, and methane was also introduced with steam through evaporator. The amount of steam was, therefore, controlled by evaporator temperature. To prevent from condensation of steam, line heater was used from evaporator to reactor inlet as sustained at 150 °C.

### 2.3. Performance test for autothermal reforming

The loading volume and weight of the disk-type Ni–Cr catalyst for the reaction were 0.74 $cm^3$ and 2.7 g, respectively. For catalytic test, the catalyst was purged with $N_2$ during the increase of reaction temperature. The produced gas was cooled to room temperature in order to remove water by a water-trapper. Analyses of the product mixtures were conducted by a micro gas

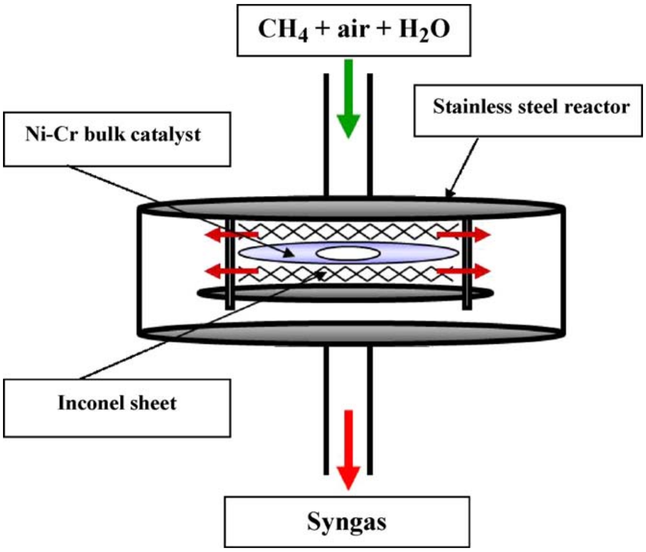

**Fig. 2.** Scheme of autothermal reformer and flow direction of gases.

chromatograph (Agilent Technology, 3000 Micro GC) with two thermal conductivity detectors which composed of a MolSieve 5A in a 10 m × 0.32 mm column to separate $H_2$, CO, $N_2$, and $CH_4$, and a PLOT U in a 3 m × 0.32 mm pre-column to separate $CO_2$ using a 1.0 μL backflush injector. Argon gas and helium gas were used for the MolSieve 5A and the PLOT U as carrier gases, respectively. For all conditions, $N_2$ was used as tie balance to calculate the methane conversion and the amount of product gases. Methane conversion was defined as follows:

$$\text{methane conversion}\,(\%) = \frac{[CH_4]_{in} - [CH_4]_{out}}{[CH_4]_{in}} \times 100$$

### 2.4. Characterization for the catalyst

The surface morphology and the sectional view of Ni–Cr disk were observed using environmental scanning electron microscopy (ESEM, FEI XL-30 FEG) and the elemental profiles in the same sample were analyzed by energy dispersion X-rays (EDX, EDAX). A detected area by EDX was 20 μm × 20 μm and the number of measurement was 25 in all samples. The crystal structures for the catalyst were measured by X-ray diffraction (D/MAX-IIIA X-ray diffractometer, Rigaku) with Cu Kα radiation. Thermogravimetric analysis (TGA 2050, TA instruments) was performed in the presence of atmosphere air and with a temperature ramp of 30 °C up to 1000 °C by 10 °C/min.

## 3. Results

### 3.1. Performance test of disk-type porous Ni–Cr bulk catalyst

Originally, an autothermal reforming is defined as the combined process of partial oxidation and steam reforming, resulting in the total reaction enthalpy of zero. In this work, we define the term of ATR as the united process of POX and SRM [20] even though the total reaction enthalpy is not zero. Many researchers have been investigated to find out the effects of $O_2$/carbon ($O_2$/C) ratio, steam/carbon (S/C) ratio, and reaction temperature to control the $H_2$/CO ratio or selectivity in methane reforming [15,21,22]. An important investigation is to determine the amount of syngas produced from methane reforming for fuel cell and the amount of $H_2$ and CO through ATR of methane was employed to estimate the performance of the Ni–Cr catalyst in this work. $H_2$ has been used as a fuel source for fuel cell, and CO could be also used as a fuel source in solid oxide fuel cell or converted to $H_2$ by a water gas shift reaction.

The performance test for the autothermal reforming of methane over the disk-type porous Ni–Cr catalyst was investigated in various conditions as represented in Figs. 3–5. But reaction temperature was limited to under 800 °C due to the thermal corrosion of the stainless steel reactor. Fig. 3 shows that the methane conversion was increased by elevating reaction temperature and by supplying higher $O_2$/C and S/C ratios. At 800 °C of Fig. 3c, methane was completely converted to syngas in S/C = 0.25 and $O_2$/C = 0.6; S/C = 0.45 and $O_2$/C = 0.5; S/C = 0.89 and $O_2$/C = 0.4. At 600 °C and 700 °C, some extent of methane remained in reformate. As a higher S/C ratio was introduced at same reaction temperature, the maximal amount of $H_2$ and CO was shown at a lower $O_2$/C ratio as following Figs. 4 and 5. When reaction temperature was elevated at same S/C ratio, the maximal product of $H_2$ and CO was also presented at a lower $O_2$/C ratio.

The reaction condition to obtain the maximal amount of $H_2$ and CO at 800 °C as shown in Figs. 4c and 5c was S/C = 0.89 → $O_2$/C = 0.2; S/C = 0.45 → $O_2$/C = 0.3; S/C = 0.25 → $O_2$/C = 0.4. A higher methane conversion as shown in Fig. 3 could be obtained by controlling the S/C and $O_2$/C ratios, but the reaction condition for the maximum product of syngas was different from the condition occurring higher methane conversion as shown in Figs. 4 and 5.

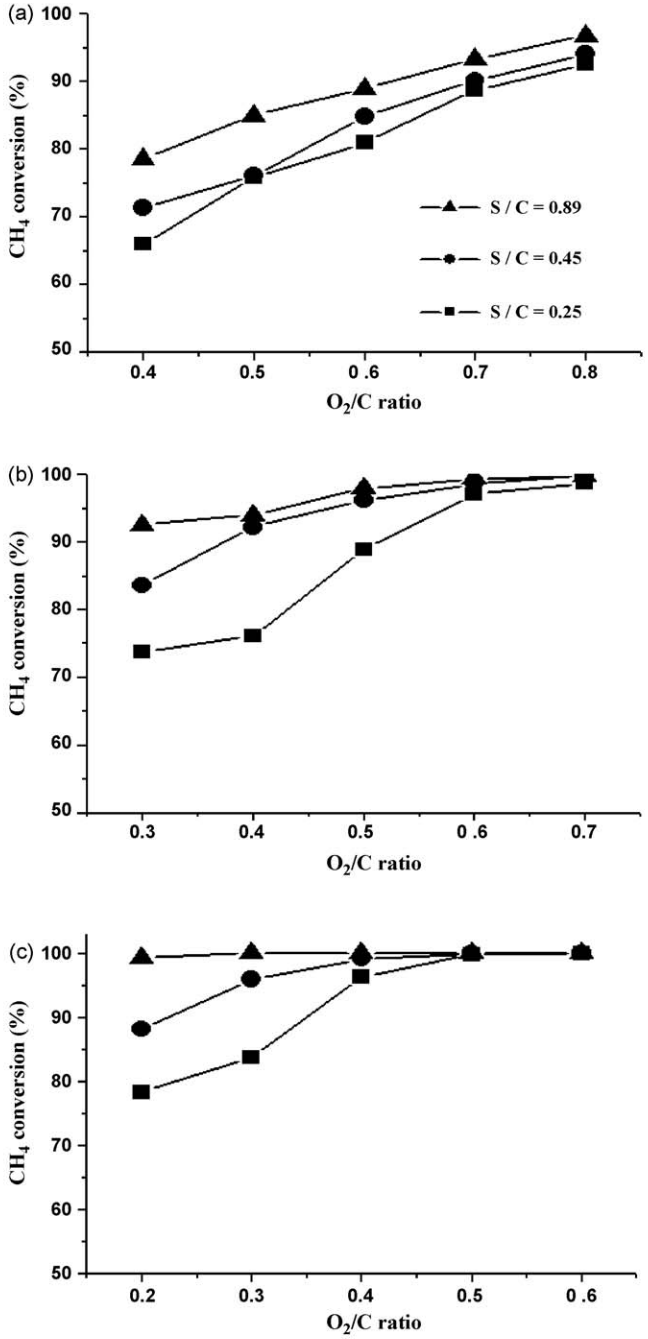

**Fig. 3.** Methane conversion in various conditions: reaction temperature; (a) at 600 °C, (b) at 700 °C, and (c) at 800 °C with 200 ml/min $CH_4$.

### 3.2. Effect of time on stream

The longevity and stability of the ATR catalyst were always a serious problem and an issued challenge. The reforming catalyst should have a physically robust property, the high methane conversion, and the high amount of $H_2$ even after conducting in a large amount of heat fluctuation such as rapid start-up and shut-down.

Fig. 6 shows the results of time on stream test. The effect of time on stream was performed under the reaction condition showing the maximal production of $H_2$ and CO at 700 °C. To confirm the

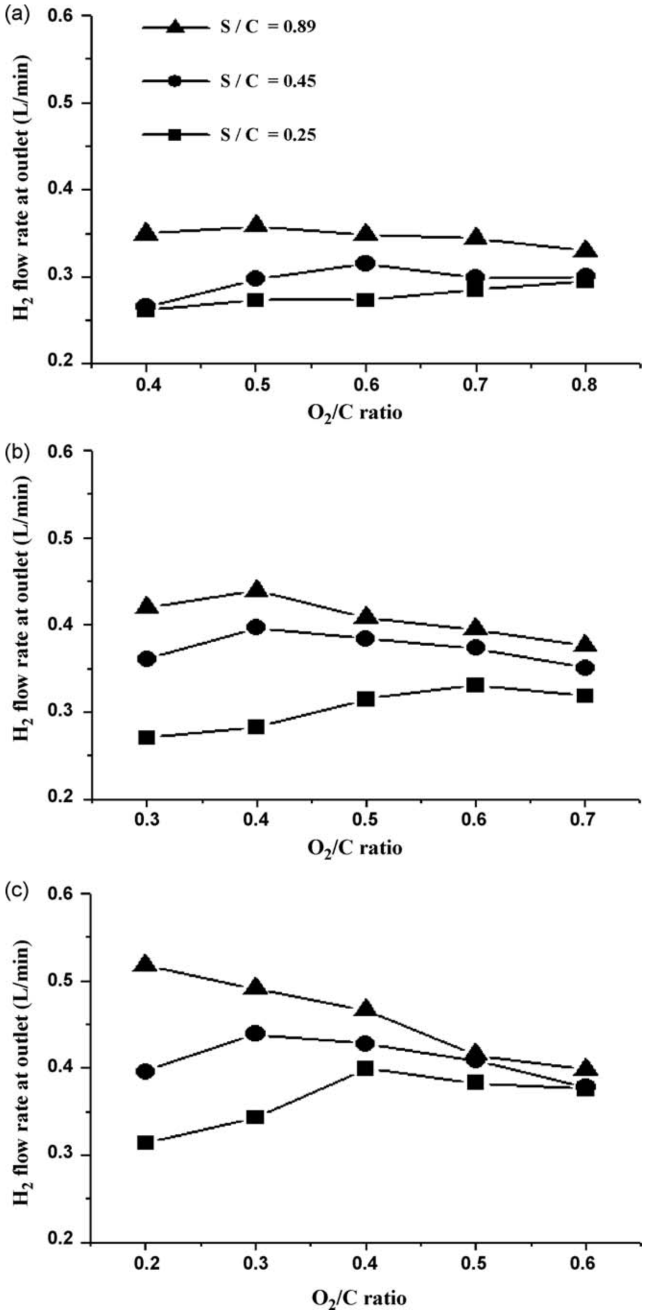

**Fig. 4.** $H_2$ production in variable conditions: reaction temperature; (a) at 600 °C, (b) at 700 °C, and (c) at 800 °C with 200 ml/min $CH_4$.

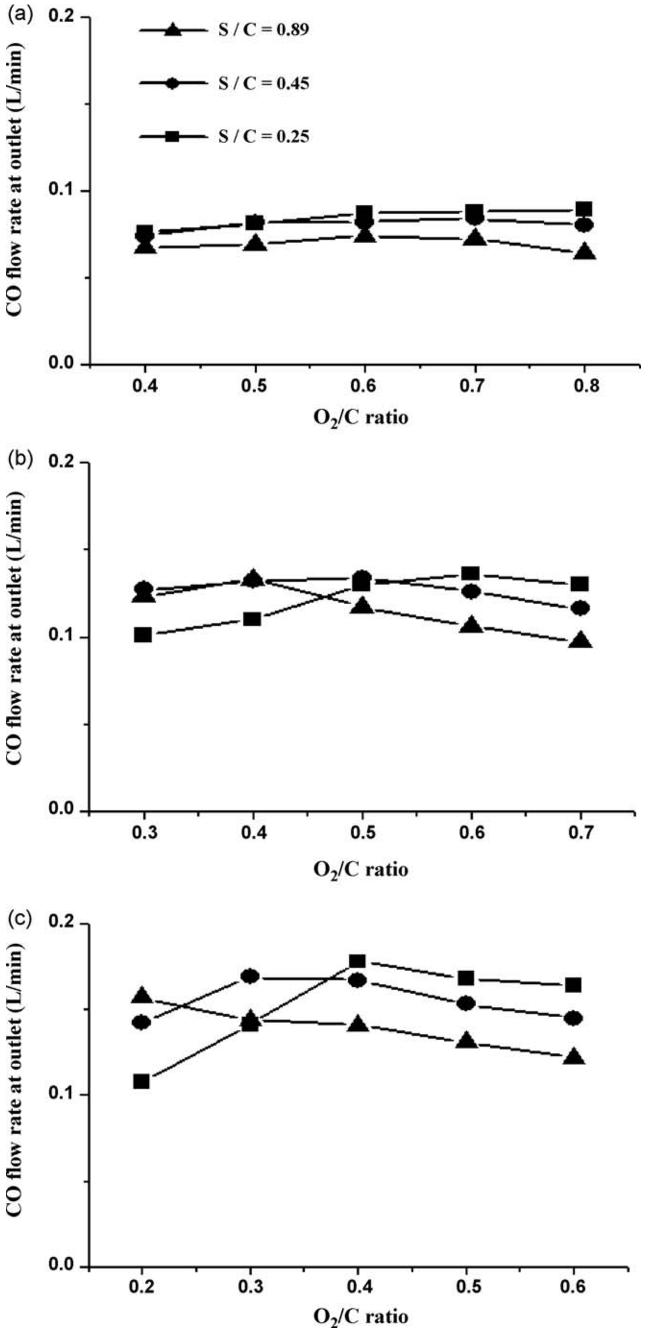

**Fig. 5.** CO production in variable conditions: reaction temperature; (a) at 600 °C, (b) at 700 °C, and (c) at 800 °C with 200 ml/min $CH_4$.

application feasibility of the Ni–Cr bulk catalyst as a reforming catalyst, the test was continuously investigated for 260 h. The initial methane conversion at 700 °C, S/C = 0.89 and $O_2$/C = 0.4 was 95%, and it was slightly decreased to 93% after 260 h as shown in Fig. 6a. In Fig. 6b, the amount of $H_2$ and CO at the reformate stream was somewhat decreased from 0.53 L/min to 0.50 L/min as well as methane conversion. From the results of time on stream, the disk-type porous Ni bulk catalyst showed sufficient feasibility to be used as a reforming catalyst.

### 3.3. On–Off test

On–Off test was introduced to understand the resistivity and stability of a reforming catalyst for oxidation at high temperature during air purge in the practical process. Each cycle of On–Off test was composed of ATR process, Off process with air purge, and On process with air purge as shown in Fig. 7. On–Off test can be depicted as follows; the reactor temperature was elevated by 5 °C/min and sustained for 24 h at 700 °C. The S/C and $O_2$/C were fixed by 0.89 and 0.4 with 200 ml/min of $CH_4$ for ATR, respectively. And then the reactor was cooled to ca. 400 °C in air atmosphere and immediately heated to 700 °C in air atmosphere without any other treatment for the catalyst such as reduction treatment by $H_2$. When the reactor temperature was reached 700 °C, air was switched to reactant gas and then ATR was carried out for 24 h with the above condition. TG analysis for the Ni–Cr catalyst in Fig. 8 was performed to confirm the On and Off conditions and the weight change of the catalyst was presented at approximately

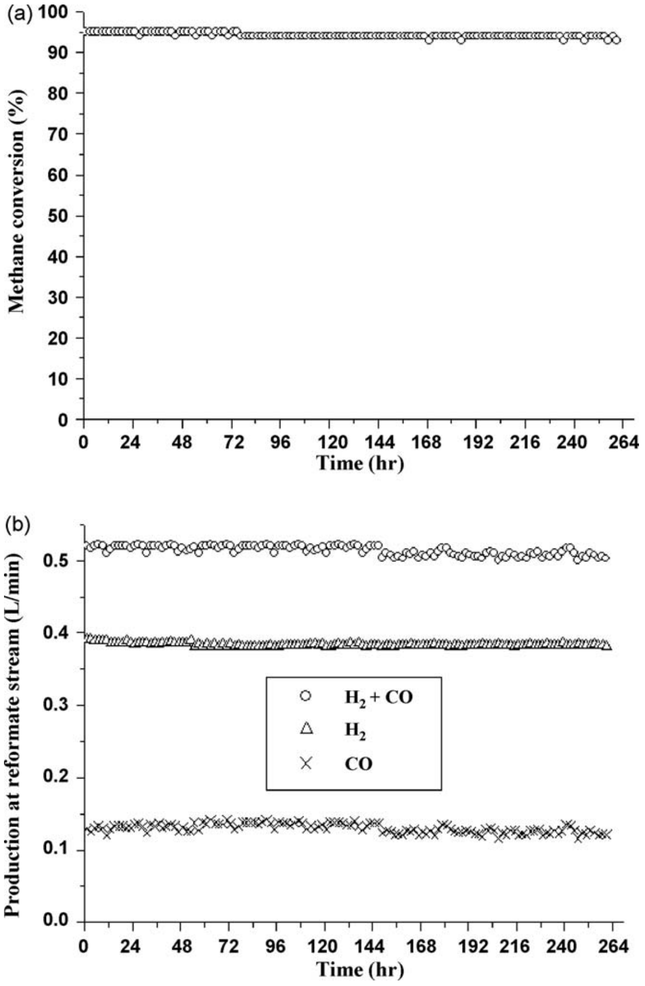

**Fig. 6.** The effect of time on stream for 260 h at 700 °C, S/C = 0.89 ($CH_4$ flow rate = 200 ml/min), and $O_2/C$ = 0.4: (a) methane conversion, (b) the amount of $H_2$ and CO production.

450 °C. The result of TG analysis showed that the catalyst was not affected by oxidation at less than 450 °C. Therefore, 450 °C was set as a minimal temperature for air purge in the On and Off conditions. The whole On–Off test was conducted for 21 cycles as shown in Fig. 9a.

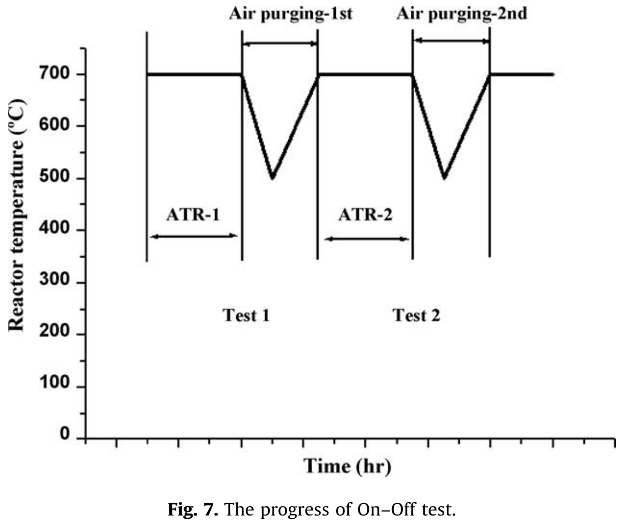

**Fig. 7.** The progress of On–Off test.

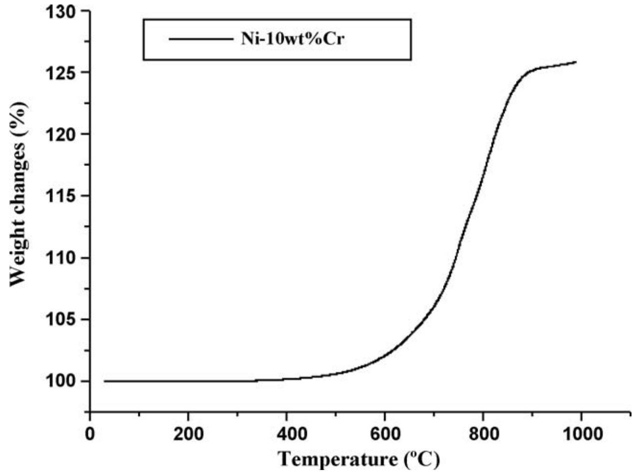

**Fig. 8.** Thermogravimetric analysis of disk-type porous Ni–Cr bulk catalyst.

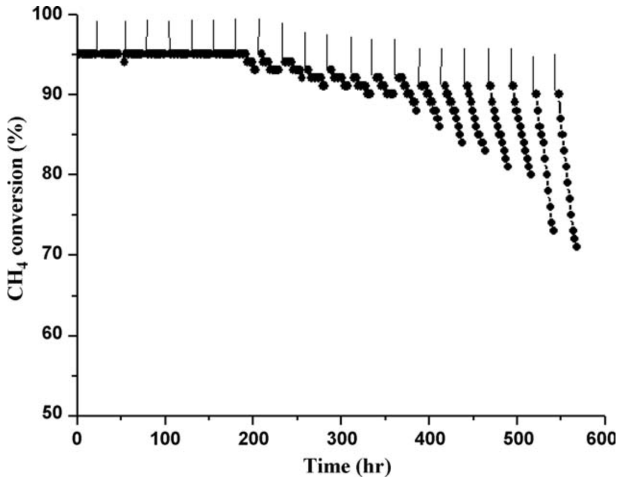

**Fig. 9.** On–Off test at 700 °C, S/C = 0.89, and $O_2/C$ = 0.4 ($CH_4$ flow rate = 200 ml/min). Mark I in this figure means the starting point of each ATR process.

95% $CH_4$ conversion had been well sustained until the seventh cycle. However, the initial $CH_4$ conversion at each cycle was slightly reduced and also the $CH_4$ conversion was changed during each ATR process after the seventh cycle in On–Off test. By repeating the number of the On–Off cycle times, the difference between the initial and final methane conversion at each ATR process was getting wider. Decreased methane conversion during the previous ATR process was not maintained in the next process

**Table 1**
The optimum condition for maximum $H_2$ and CO production in autothermal reforming of methane.

| Reaction temperature | Maximum condition | |
|---|---|---|
| | S/C ratio | $O_2/C$ ratio |
| 600 °C | 0.25 | 0.8 |
| | 0.45 | 0.6 |
| | 0.89 | 0.5 |
| 700 °C | 0.25 | 0.6 |
| | 0.45 | 0.4 |
| | 0.89 | 0.4 |
| 800 °C | 0.25 | 0.4 |
| | 0.45 | 0.3 |
| | 0.89 | 0.2 |

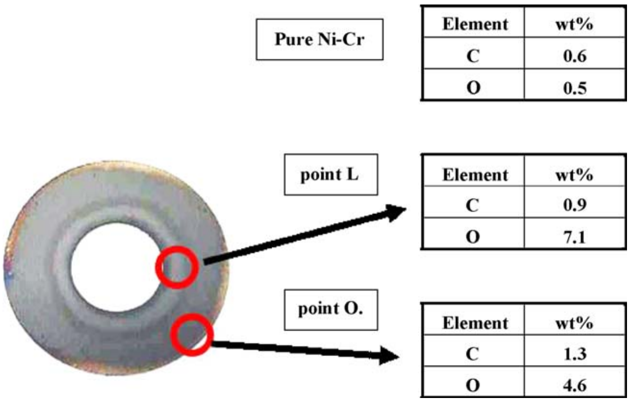

Pure Ni-Cr

| Element | wt% |
|---|---|
| C | 0.6 |
| O | 0.5 |

point L

| Element | wt% |
|---|---|
| C | 0.9 |
| O | 7.1 |

point O.

| Element | wt% |
|---|---|
| C | 1.3 |
| O | 4.6 |

**Fig. 10.** EDX analysis of disk-type porous Ni–Cr catalyst after 260 h at 700 °C, S/C = 0.89 ($CH_4$ flow rate = 200 ml/min), and $O_2/C$ = 0.4.

and it was bounced to a higher methane conversion than the final methane conversion in the previous ATR process.

## 4. Discussion

### 4.1. The optimal condition in autothermal reforming of $CH_4$

Table 1 shows the optimal conditions to generate the maximal amount of $H_2$ and CO. $H_2$ and CO are products of partially oxidized methane reacted with steam and oxygen. The more methane converted, the more $H_2$ and CO might be generated. To increase the methane conversion, the effect of reaction temperature, S/C ratio, and $O_2/C$ ratio was investigated and the results are shown in Fig. 3. However, the optimal condition producing the maximal $H_2$ and CO quantity was different from the condition producing the higher methane conversion. The optimal condition was originated by the extent of progress between the complete oxidation and the partial oxidation of methane as presented in Figs. 4 and 5. As $O_2/C$ ratio is higher than the optimal condition, the methane conversion will increase, but the produced amount of $H_2$ and CO may decrease. From Table 1, the optimal conditions as increasing reaction temperature and S/C ratio were shifted to a lower $O_2/C$ ratio. It indicates that methane converted at high $O_2/C$ ratio is oxidized to $H_2O$ and $CO_2$ rather than $H_2$ and CO by excessive $O_2$, as reported elsewhere [23].

### 4.2. Deactivation of porous Ni–Cr bulk catalyst in ATR

As mentioned already, an Ni bulk catalyst was not useful in the reforming reaction due to its physical instability in a severe reforming condition. Meanwhile, the disk-type porous Ni–Cr bulk catalyst showed stable activity during autothermal reforming as presented in Fig. 6. The catalyst surface was, however, slightly deactivated during the 260 h operation. EDX results in Fig. 10 showed that the amounts of oxygen and carbon on the catalyst surface increased and was constant after the 260 h operation of ATR, respectively. It indicates that an active Ni was deactivated by oxidation of the catalyst and lost its activity. SEM images at points I and O of Fig. 11 represent that the morphology changes of the Ni–Cr catalyst surface were caused absolutely not by carbon but by the oxidation of Ni. The NiO peak presented after the reaction in XRD analysis of Fig. 12b could be another evidence of the catalyst deactivation by the Ni oxidation.

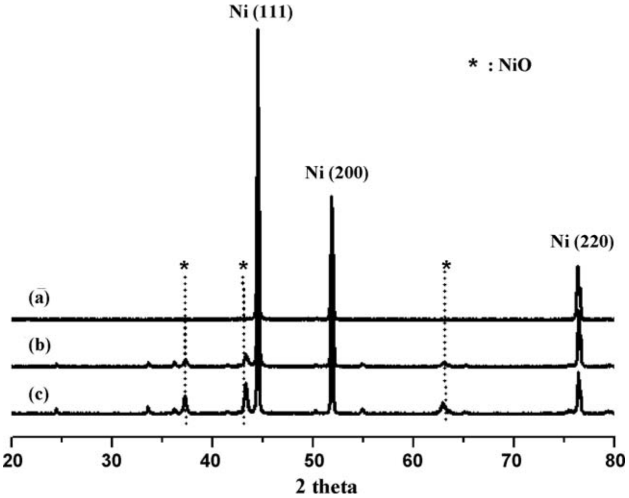

**Fig. 12.** XRD analysis of disk-type porous Ni–Cr catalyst: (a) pure Ni–Cr, (b) after 260 h ATR of methane, and (c) after On–Off test.

Generally, the catalyst deactivation in a reforming reaction is ascribed by carbon deposition on the active Ni sites. However, the deactivation of the Ni–Cr bulk catalyst had been occurred by oxidation of active Ni sites because the carbon formation can be easily suppressed by oxygen [21] and steam [24,25] in ATR of methane. Since Ni oxidation is much faster than the reforming reaction [15], NiO was gradually abundant on the Ni–Cr bulk catalyst at oxygen-rich atmosphere and it contributed to the catalyst deactivation [20,26] even though Ni can be easily reduced by methane decomposition.

EDX results of the cross-section of the catalyst in Fig. 13 show that the reactant gas was well diffused into the porous Ni–Cr disk and the overall region of the disk-type porous Ni–Cr catalyst had been used to reform methane to syngas.

### 4.3. Bounce phenomenon

The results of On–Off test in Fig. 9 show an interesting fact, which is named as bounce phenomenon in this work. The bounce

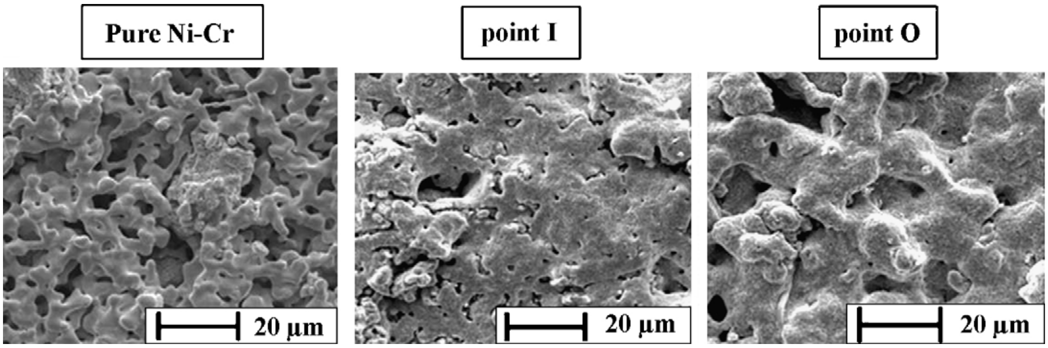

**Fig. 11.** SEM images of disk-type porous Ni–Cr catalyst after 260 h at 700 °C, S/C = 0.89 ($CH_4$ flow rate = 200 ml/min), and $O_2/C$ = 0.4.

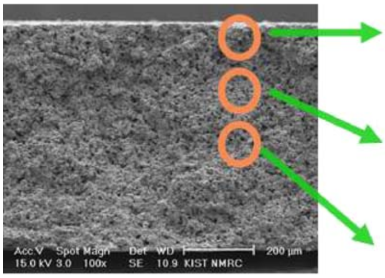

| Element | wt% |
|---|---|
| C | 1.0 |
| O | 3.0 |

| Element | wt% |
|---|---|
| C | 2.1 |
| O | 3.5 |

| Element | wt% |
|---|---|
| C | 1.5 |
| O | 3.6 |

**Fig. 13.** EDX analysis of cross-section of disk-type porous Ni–Cr catalyst after 260 h at 700 °C, S/C = 0.89 ($CH_4$ flow rate = 200 ml/min), and $O_2/C$ = 0.4.

phenomenon indicates that the Ni bulk catalyst oxidized during the reaction and the air purge step reduced Ni metal by methane decomposition and the activity of the Ni catalyst bounced back closely to the initial state.

$$\text{Methane decomposition and Ni reduction}: \ \mathrm{Ni{-}O} + \mathrm{CH_4} = \mathrm{CO} + 2\mathrm{H_2} + \mathrm{Ni}$$

In Fig. 9, the decreased Ni activity was not continued at the next cycle. The initial activity of the catalyst at each cycle after the seventh cycle decreased gradually by the deactivation of the bulk Ni catalyst. The oxidation of Ni is the main reason causing the decrease of initial activity at each cycle after seventh cycle. A pore block of the catalyst surface proceeding gradually by the oxidation of Ni reduced the catalytic activity at the initial state of each ATR process and may prevent the reactant gases from diffusing to the inside of the catalyst. Nevertheless, the bounce of catalytic activity appeared repeatedly. The catalytic activity during each ATR process was reduced by a catalyst deactivation through Ni oxidation and was recovered transiently by the reduction to Ni metal through methane decomposition.

## 5. Conclusions

The application of the disk-type porous Ni–Cr bulk catalyst on autothermal reforming of methane was successful, and the catalytic activity was also sufficient. We can conclude from the results that the development of a compact autothermal reformer is feasible by using the disk-type porous Ni–Cr bulk catalyst. The optimal condition for maximal $H_2$ and CO production could be controlled by the reaction conditions because the purpose of syngas generation for fuel cell is focused on gaining a vast amount of $H_2$ and CO. In 260 h of operation of ATR and On–Off test, the catalyst deactivation by carbon coking did not occur, but the deactivation by oxidation of Ni was an inevitable result. More studies on preventing the catalyst deactivation should be further researched in future works.

## Acknowledgements

This work was financially supported by Center for Fuel Cell Research of Korea Institute of Science and Technology, and by the ERC program of MOST/KOSEF (Grant No. R11-2002-102-00000-0).

## References

[1] J.R. Rostrup-Nielsen, I. Dybkjaer, K. Aasberg-Petersen, Prep. ACS Petr. Chem. Div. 45 (2) (2000) 186.

[2] J.R. Rostrup-Nielsen, Catal. Today 71 (2002) 243.

[3] J.-H. Kim, H.-I. Lee, Korean J. Chem. Eng. 21 (1) (2004) 116.

[4] S. Kim, I. Hong, J. Ind. Eng. Chem. 14 (2008) 357.

[5] D.P. Chynoweth, Renew. Energy 22 (2001) 1.

[6] C. Courson, A. Kiennemann, Catal. Today 76 (2002) 75.

[7] M.A. Pena, J.L.G. Fierro, Appl. Catal. A 144 (1996) 7.

[8] J.N. Armor, Appl. Catal. A 176 (1999) 159.

[9] J.-S. Choi, J.-S. Yun, H.-H. Kwon, T.-H. Lim, S.-A. Hong, H.-I. Lee, J. Power Sources 145 (2005) 652.

[10] Y. Matsuo, Y. Yoshinaga, Y. Sekine, K. Tomishige, K. Fujimoto, Catal. Today 63 (2000) 439.

[11] T. Rampe, A. Heinzel, B. Vogel, J. Power Sources 86 (2000) 536.

[12] K.-Y. Kim, J. Han, S.W. Nam, T.-H. Lim, H.-I. Lee, Catal. Today 131 (2008) 431.

[13] B.F. Hagh, Int. J. Hydrogen Energy 28 (2003) 1369.

[14] S. Ayabe, K. Eguchi, Appl. Catal. A 241 (2003) 261.

[15] M.M.V.M. Souza, M. Schmal, Appl. Catal. A 281 (2005) 19.

[16] S.-B. Tang, S.-J. Lu, Catal. Today 24 (1995) 253.

[17] D.L. Trimm, Catal. Today 37 (1997) 233.

[18] A. Shamsi, Appl. Catal. A 277 (2004) 23.

[19] S.H. Kim, S.W. Nam, T.-H. Lim, H.-I. Lee, Appl. Catal. B 81 (2008) 97.

[20] T. Takeguchi, S.-N. Furukawa, M. Inoue, K. Eguchi, Appl. Catal. A 240 (2003) 223.

[21] J.A.C. Dias, J.M. Assaf, J. Power Sources 137 (2004) 264.

[22] E.C. Wanat, K. Venkataraman, L.D. Schmidt, Appl. Catal. A 276 (2004) 155.

[23] Y.-S. Seo, A. Shirley, S.T. Kolaczkowski, J. Power Sources 108 (2002) 213.

[24] T. Furusawa, A. Tsutsumi, Appl. Catal. A 278 (2005) 207.

[25] D.C. Gardner, C.H. Bartholomew, Ind. Eng. Chem. Prod. Res. Dev. 20 (1981) 80.

[26] S. Ayabe, H. Omoto, T. Utaka, R. Kikuchi, K. Sasaki, Y. Teraoka, K. Eguchi, Appl. Catal. A 241 (2003) 261.